

# Acoustic Local Positioning System Using an iOS Device

T. Aguilera\*, J. A. Paredes, F. J. Álvarez and J. I. Suárez  
Department of Electrical Engineering, Electronic and Automatic  
University of Extremadura  
Badajoz, Spain, 06006  
\*Email: teoaguibe@unex.es

A. Hernández  
Electronics Department  
University of Alcalá  
Alcalá de Henares, Spain, 28871  
Email: alvaro@depeca.uah.es

**Abstract**—This work benefits from the capability of the iPhone's or iPad's microphone to acquire high-frequency sound for accurate acoustic code identification. Although the maximum theoretical value for the frequency response of the built-in iOS device microphone is 20 kHz, emissions with frequencies close to 22 kHz have been experimentally detected. The frequencies used in this work are in the range from 18 to 22 kHz, which are high enough to be inaudible for almost every people but low enough to be generated by standard sound hardware.

The aim of this work is to develop an inexpensive indoor positioning system where the user gets its location by using an iOS device's microphone. For this purpose a third-generation iPad is used for high-frequency sound data acquisition and neither external acquisition system nor ultrasonic microphone are required.

The capability of iOS devices to acquire acoustic signals in the vicinity of 20 kHz has been successfully demonstrated. This fact allows the use of this kind of device for acoustic code detection and accurate positioning by means of multilateration.

**Keywords.** Local Positioning System; iOS Device; Kasami Codes; CDMA; Objective-C Application.

## I. INTRODUCTION AND RELATED WORKS

Everybody is aware about the growing spread and computational power of mobile phones and the rising number of applications (apps) we find in app stores, full of different location-based apps such as restaurant finders, tourist guides and navigation systems, etc. Since smartphones and wireless Internet connection became ubiquitous in the last years, location based interaction, supported via the Global Positioning System (GPS) or WiFi identification has become a standard pattern for mobile phone usage.

Nowadays most smartphones are equipped with a GPS receiver, which raises costs and increases the energy consumption. Unfortunately, GPS is not able to track people in indoor environments with acceptable accuracy [1]. Signals might get lost due to attenuation effects of roofs and walls or lead to position fixes of very low accuracy due to multipath propagation. Therefore, GPS is not a good option for indoor location currently.

Works as the one presented in [2] propose a system based on infrared receivers (IR), distributed inside the building, and a device sending IR signals. Unfortunately, smartphones generally do not integrate an IR emitter, a complex and costly infrastructure has to be built. The same problem presents

Magnetic Indoor Positioning System (MILPS) [3] [4] which uses artificial magnetic fields generated by coils for ranging between multiple coils and a mobile station equipped with a magnetic sensor. Other option is to use Bluetooth receivers [5], which are integrated in many mobile devices, but unfortunately access to it is often limited by the operating system.

A different approach is to use position information deduced from a combination of Global Navigation Satellite System (GNSS) where available, combined with Pedestrian Dead Reckoning (PDR) utilizing inertial measurements and context-aware activity based map matching [6] [7]. Unluckily experiments have shown that several sources of error accumulation exist, being the most important the heading error.

Other works [8]–[10] propose the use of WiFi signals to perform such a localization, but absorption and reflection generate confusion [11] and the required WiFi parameters cannot always be accessed on modern phones operating systems.

An attractive possibility is to triangulate the device position using ultrasonic signals [12]–[15]. These works use frequencies and algorithms which require special hardware on the client side. A compromise is the use of ultrasonic frequencies close to the human perceiving threshold (i. e. around 20 kHz) to identify the presence of a beacon sender [16]. Taking into account that audio recording is a standard smartphone feature, and that smartphone microphones are capable to sense sound on ultrasonic frequencies close to 22 kHz, this work presents an approach for inexpensive and easy indoor positioning which can be carried out with the help of a mobile device or tablet using its built-in microphone as receiver [17]. The positioning algorithm can be implemented locally on the user's device, if a particular set of signals and their origin positions (beacons) are known to the device. This requires the device to access a beacon map, which must be maintained for every site.

The purpose of this work is to use the good correlation and cross-correlation properties of Kasami codes [18] for indoor sound multilateration positioning. At the same time, ultrasonic signals can be used to sense the proximity of a beacon, offering useful information related with beacon's location. In this case, errors should not exceed a few meters, otherwise, the service could provide information for places which are quite far away from the actual position of the target.

Such information can be displayed via a webpage, building plan, sound message...etc. A possible implementation based on ultrasonic technology of those indoor services could be carried out in a museum tour guide [19]. Systems currently used in museums provide unsophisticated functionality which is very often limited to manually entering a number in order to hear a recording. Indoor location based services require higher precision guarantees than outdoor services. Nowadays the state of the art for indoor LBS and context-sensitive services is still an outstanding problem.

The remainder of the paper is structured as follows: in the next section, the algorithms used for Kasami codes generation and multilateration are presented, followed by a description of the general system design in the third section. The system has been evaluated on-site, the results are analyzed in the fourth section. To conclude, a recapitulation of the main contributions of this work, together with a description of the next steps and further improvements are shown in the fifth section.

## II. THEORETIC CONCEPTS

### A. Kasami Codes

In this work we take advantage of the ability of the iPhone's or iPad's microphone to acquire high frequency sound for accurate code identification. The signals emitted are 255-bit Kasami sequences with BPSK modulation at 20 kHz. This kind of sequences belongs to the well known family of pseudorandom codes [20].

A Kasami sequence  $k$  can be generated from a maximal sequence and the decimated and concatenated version of this sequence by performing the module-2 sum of the former with any delayed version of the latter, i.e.,

$$k = m_1 \oplus D^l m_2 \quad (1)$$

where  $m$  is a maximal sequence of length  $L = 2^{N-1}$  with  $N$  even,  $m_2$  is the sequence obtained from the decimation of  $m_1$  with a decimation factor of  $q = 2^{N/2} + 1$  and the concatenation of the result  $q$  times,  $\oplus$  represents the module-2 sum and  $D^l m_2$  is the sequence obtained by cyclically shifting  $l$  positions the  $m_2$  sequence.

In order to adapt the spectral features of the emission to the frequency response of the ultrasonic emitter, these codes are binary phase modulated (BPSK). This modulation scheme has been widely used to transmit binary codes in matched filtering-based sonar systems. Every bit in the code  $k[n]$  is modulated with one or more carrier cycles whose phase, 0 or  $\pi$ , is given by the bit value to obtain the modulated pattern as:

$$p[n] = \sum_{i=0}^{l-1} k[i] \cdot m[n - i \cdot N_c \cdot M] \quad (2)$$

where  $L$  is the code length,  $m[n]$  is the modulation symbol formed by  $N_c$  carrier cycles, and  $M$  represents the number of samples per period (ratio between the sampling and the carrier frequencies).

### B. Multilateration Algorithm

To resolve the user's location a multilateration has been used. This technique involves measuring the time difference between a captured signal, emitted by a beacon and other signals captured subsequently emitted by the remaining beacons. With the information obtained from the distance measurements and the knowledge of the beacon's location, we propose a system of equations that solves the user's position. Fig. 1 shows a graphic representation for multilateration technique.

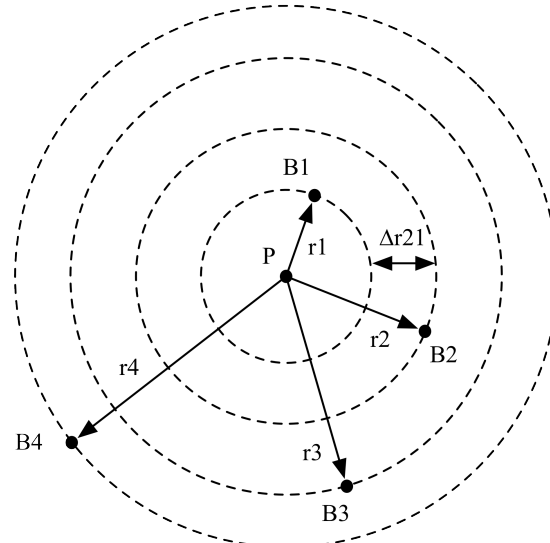


Fig. 1. Approach for multilateration technique.

In Fig. 1  $B_i$  ( $i = 1 \dots 4$ ) are the positions of the ultrasonic beacons which are known and  $P$  is the user's location which we want to estimate. On the other hand  $\Delta r_{i1}$  is the distance difference between beacon  $i$  and 1 from the user's position  $P$ .

To solve the user's location the Gauss-Newton algorithm is used. The Gauss-Newton algorithm is an iterative method regularly used for solving nonlinear least squares problems. The procedure consists of a sequence of linear least squares approximations to the nonlinear problem, each of which is solved by an iterative process.

The algorithm starts from a close and approximate position  $(\hat{x}, \hat{y}, \hat{z})$  of the user and uses iterations to minimize the sum of squared errors of the distances  $F(x, y, z)$  to estimate the user's position, where:

$$F(x, y, z) = \sum_{i=2}^4 (\hat{r}_{i1} - r_{i1})^2 \quad (3)$$

This process works until getting an estimation of the user's position  $(x, y, z)$  in which the squared error  $(\Delta x, \Delta y, \Delta z)$  is sufficiently small. Finally the user's position is estimated as:

$$P(x, y, z) = (\hat{x}, \hat{y}, \hat{z}) - (\Delta x, \Delta y, \Delta z) \quad (4)$$

### III. SYSTEM DESIGN

#### A. Hardware

A diagram showing the full system is depicted in Fig. 2. Such diagram shows the connections between the different elements composing the system.

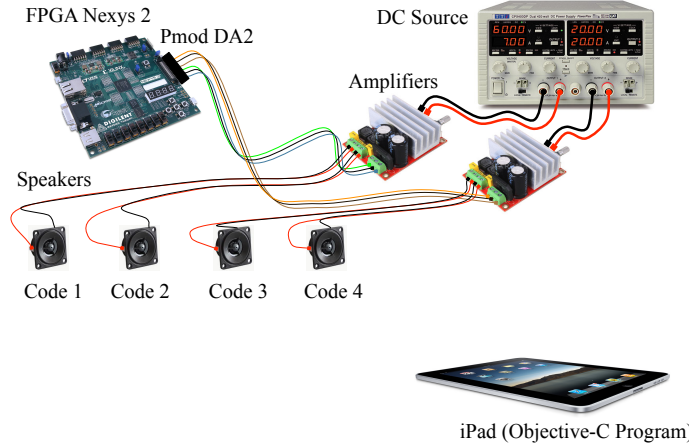


Fig. 2. Connection diagram of the whole system.

The codes were synthesized by means of a *Nexys 2* FPGA-based board which has been programmed to simultaneously generate four different Kasami codes that are periodically emitted with an interval of 50ms between emissions. These digital signals are converted to analog with the help of two double digital to analog converter modules (*Digilent PmodDA2*). After that, signals are transmitted to the audio amplifiers (*Philips TDA8920BTH*) which are powered by means of a DC source in order to drive a set of four speakers (*Visaton SC5*). Once the codes have been emitted, they are acquired and processed by the *iPad*, using its own built-in microphone and finally the device identifies these codes by matched filtering.

Beacons have been placed in different positions inside our laboratory, whose dimensions are  $5.75 \times 5.50 \times 3.00$  meters. To measure the beacon's positions a laser rangefinder (*Bosch GLM80*) is used which has a  $\pm 1$  mm of error. Fig. 3 shows the distribution of the beacons in the working environment.

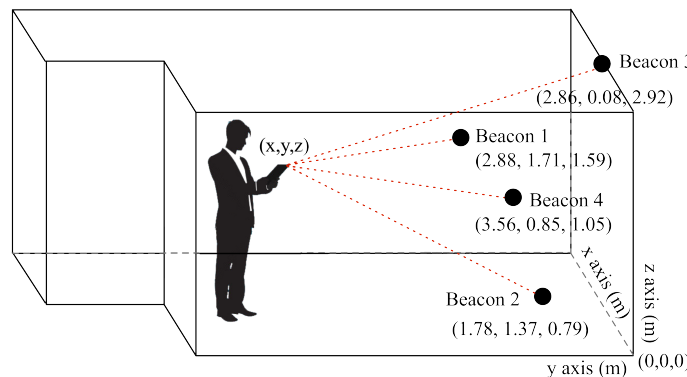


Fig. 3. Beacons distribution.

#### B. Software

To acquire audio with an *iOS* device is necessary to implement and configure the *Audio Queue Services*, which is a C programming interface in *Core Audio Toolbox* framework, available through *The Mac Developer Library* [21]. System frequency acquisition was chosen as 48 kHz and buffers capabilities were set to 3624 samples, this implies that every 75.5 ms the program saves data from the buffer to a pointer in memory.

The data acquisition process is described in Fig. 4.

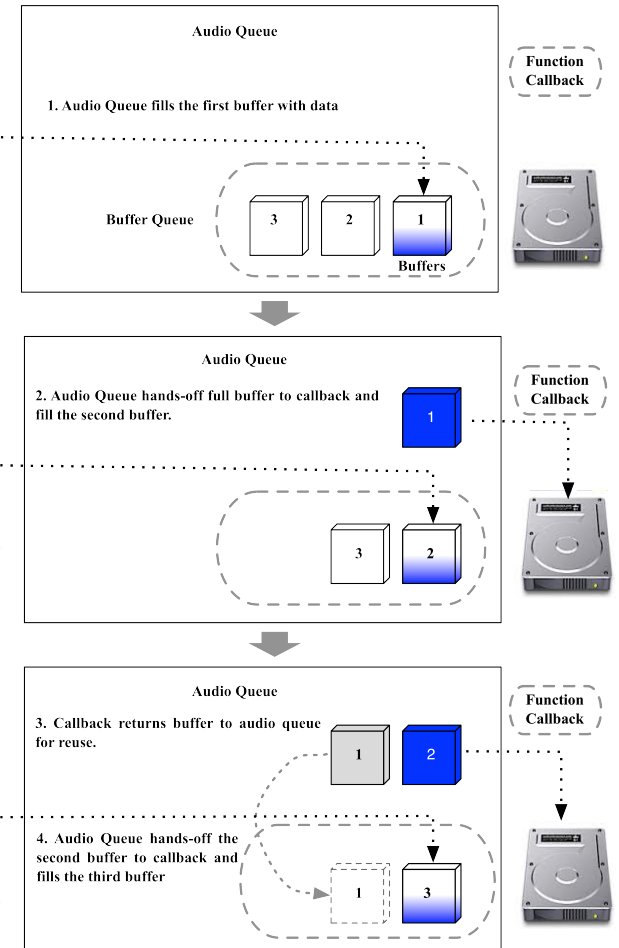


Fig. 4. Data acquisition process.

After that, these samples are processed by means of the *vDSP API* which provides mathematical functions for applications involving data processing. This utility allows: (1) the identification of the emitted codes by performing a matched filtering, (2) the correlation peak detection by thresholding and (3) the computing of the time-of-flight-differences (DTOF) to determine the distances to the beacons.

Finally the user's location is carried out by means of the multilateration algorithm implemented on the *iPad* and whose operation was described in detail in section II B .

#### IV. EXPERIMENTAL RESULTS

##### A. Frequency Response

Since modern smartphones allow to record sound with 48 kHz sample rate, is technically possible to detect sounds with a maximum frequency of 24 kHz according to the Nyquist-Shannon theorem. Also, modern smartphone microphones are well able to record sounds up to this frequency, offering a spectrum of about 4 kHz above the human reception which is high enough to be inaudible for almost every people.

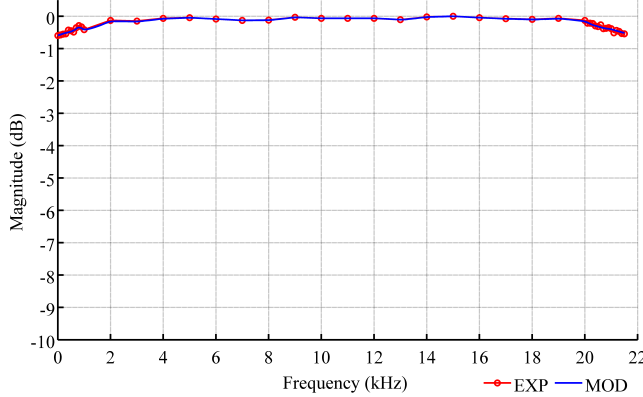


Fig. 5. Frequency response.

Fig. 5 shows the frequency response of the receiver when is located at one meter in the acoustic axis of one of the speakers, emitting sinusoidal signals at different frequencies. Besides a 50-tap IIR filter has been designed to simulate the system behavior.

##### B. Signal Processing

To avoid hearing the transient effects produced between emissions, some additional signal processing has been necessary. Figs. 6 a) and b) show the behavior of *Code1* before and after to carry out a band-pass filtered together with a Hamming-windowed respectively. After this treatment transient effects are so attenuated that they result inaudible, unless very sensitive people get really close to the speaker.

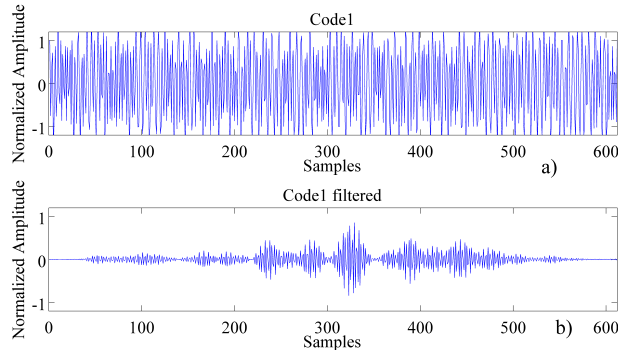


Fig. 6. Signal processing of *Code1*.

##### C. Data Acquisition and Processing

The data are captured by the 32-bit Analogic-to-Digital Converter (ADC) integrated in the *iPad*. Since the length of the codes are 612 samples and a period of time of 50 ms exists between emissions (2400 samples at 48 kHz sample rate), the buffer capacity has been set to  $612+2400+612 = 3.624$  samples to ensure that at least a package of four Kasami codes, which are emitted simultaneously, is captured into every buffer.

Fig. 7 a graphic representation of the data stored into the audio buffer.

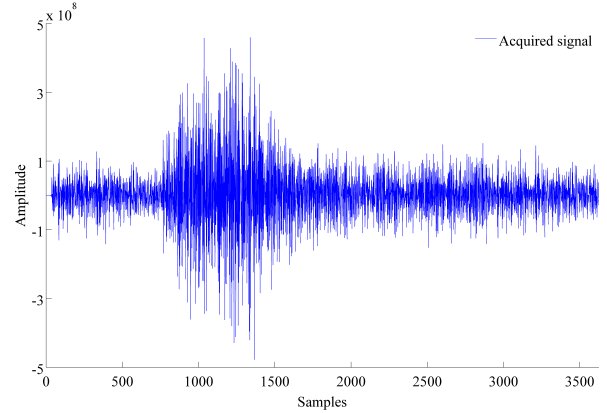


Fig. 7. Acquired signal.

Once the codes have been acquired they are processed by the *iPad*, which identifies the codes performing a cross correlation between the acquired signal and the emission patterns. Fig. 8 represents the overlapped results for the four cross-correlations where are distinguishable the correlation peaks belonging to the four emitted codes. These correlation peaks determine the TOF from each of the beacons to the *iPad* and thus the distance to each one. From these distances the user's position is estimated with the help of the already described multilateration algorithm.

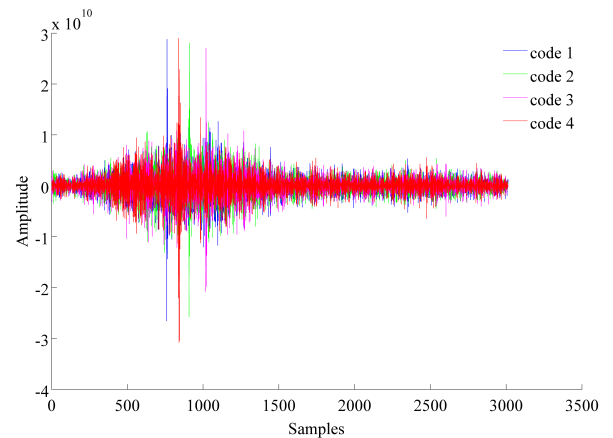


Fig. 8. Overlapped cross correlation results.

#### D. Accuracy and Reliability

To assess the accuracy and reliability of the positioning system, we have taken the user's position on certain zones. To measure the accuracy of the system a set of points were chosen where the system could present problems (corners, close to walls, far points...etc). A total of five points were selected and one hundred measurements were taken from each of these positions, to evaluate the reliability of the measurements. Fig. 9 represents the coordinates of the selected points.

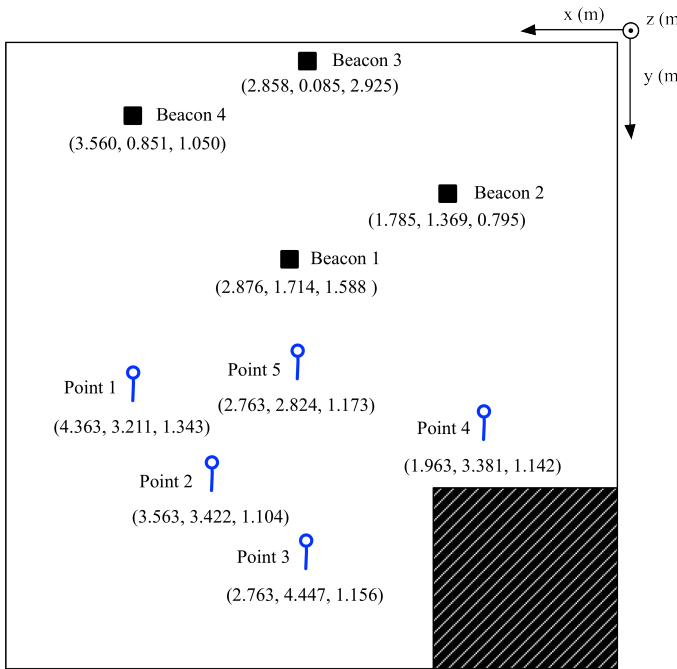


Fig. 9. Locations of tested points.

The position of *Point 1* has been chosen because of its proximity to one of the side walls (left). The reason for this choice is to check how the reception of the codes in that position is affected by the directivity pattern of the speakers. On the other hand, *Point 2* is an intermediate position among *points 1, 3 and 5*, and was chosen to compare its results with these points. *Point 3* is centered, at an appropriate distance from the beacons and walls, to prevent near-far effect and multipath respectively. With the election of this point, we are looking for a location having the best conditions to be located with the best possible accuracy. Then *Point 4* is located in the proximity of a corner, we choose these coordinates to study how multipath affects the reception of the emissions. Finally *Point 5* is situated near *Beacon 1*, where the receiver captures a strong signal coming from the nearest beacon, and thereby making it impossible to detect others weaker signals from the remaining beacons (near-far effect).

Fig. 10 depicts the five points studied, the beacon's locations and the estimated user's positions. We eventually considered representing a cenital view since *x* and *y* coordinates are the most relevant and the results are more clearly exposed.

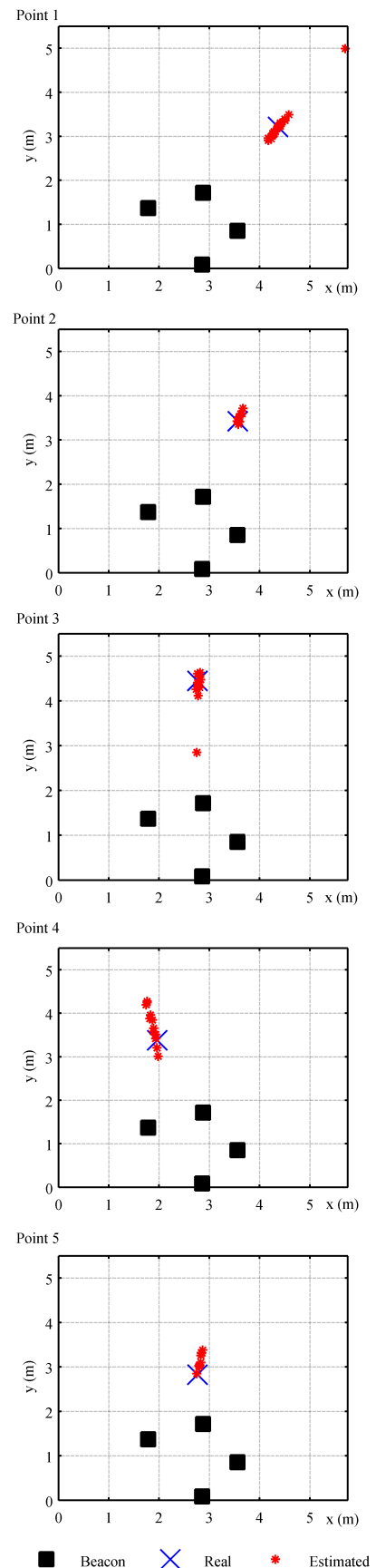


Fig. 10. Cenital view with the results obtained in the test points.

A statistical study of the positioning errors have been also carried out. Fig. 11, shows the CDF of the error measured in the five test points for the three coordinates.

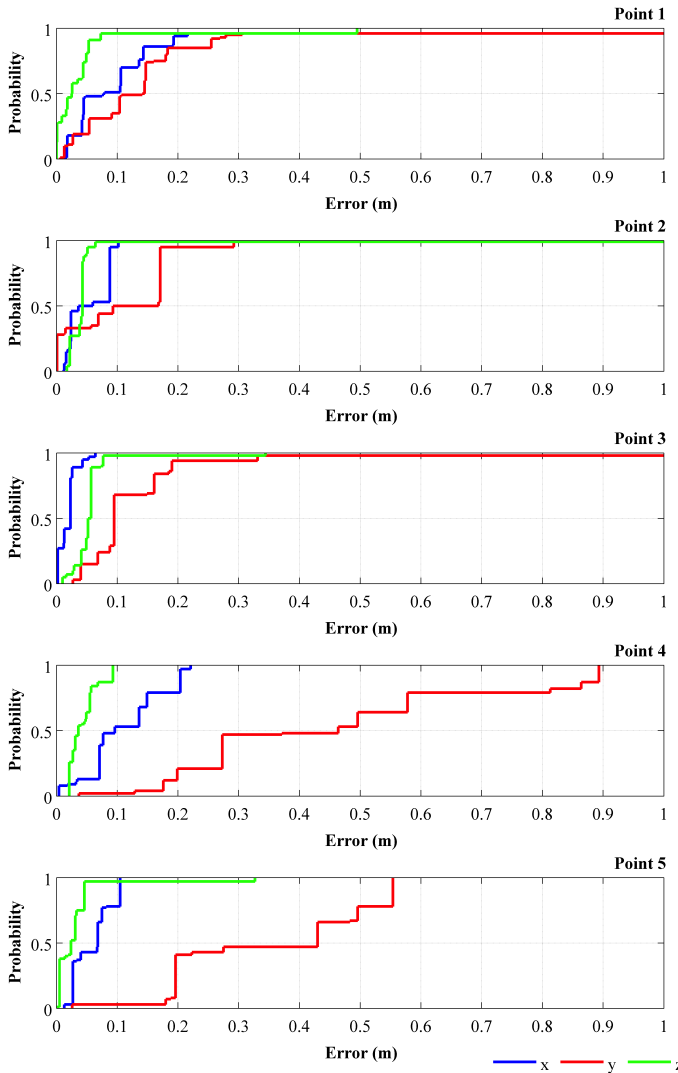


Fig. 11. Cumulative distribution function of the error.

According to Fig. 11, the first three points present the best results, with error less than 0.3 m in all cases for the three coordinates.

As expected, *Point 3* presents the lowest error of the five points because is less affected by multipath and the near-far effect than the rest of the points. Looking into its CDF, it can be observed that a 100% of probability exists that the measurements have errors below 0.10 meters for *x,z* coordinates, and 70% for *y* coordinate.

Moreover, *Point 2* has worse results than *Point 3* but slightly better than *Point 1*. Both cases, *Point 1* and *2*, the errors for the three coordinates are lower than 0.30 meters with a 100 % of probability, however *Point 2* is more likely to have a lower magnitude of the error.

On the other hand, *Point 4* and *5* have worse results than the first three points, especially *Point 4*. This point is located near a corner, therefore is strongly affected by multipath propagation. Multipath is the most dominant error source for positioning because it has a large influence on the positioning accuracy due to the received signals are disturbed by reflections. This can lead to a large bias in the user's TOF value. As shown the CDF graph of the error for *Point 4*, the results obtained are clearly inaccurate, especially for the *y* coordinate, where 0.9 meter errors exist in some cases.

Finally the results obtained for *Point 5* are also quite imprecise. This time the source of error is the near-far effect due to the proximity between the *Beacon 1* and the receiver. The result shows that exists errors lower than about 0.6 meters for the *y* coordinate with a 100% of probability.

As said, near-far effect is produced when the receiver captures a strong signal provenient from a close beacon and makes impossible the detection of other weaker signals provenient from the rest of the beacons. When this phenomenon happens, the peak of correlation corresponding with the code which is emitted by the closer beacon to the receiver, presents a clearly higher value. Fig. 12 depicted this phenomenon when occurs in *Point 5*.

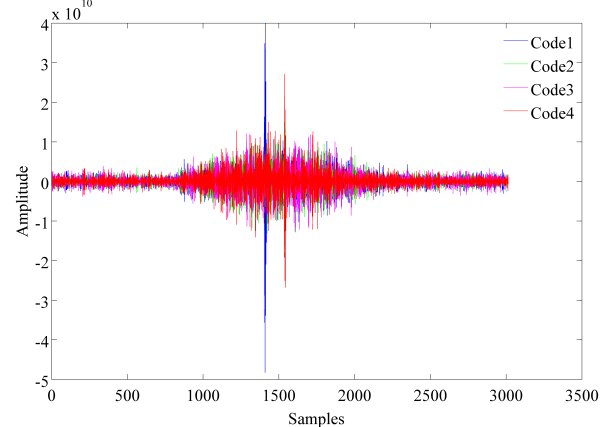


Fig. 12. Near-far effect in *Point 5*.

Although this phenomenon causes errors in the determination of the TOF, this fact can be exploited to detect the user proximity to the beacon. Also, the beacon's location could be related with useful information for the user, providing him Location-Based Services (LBS).

### E. User Interface

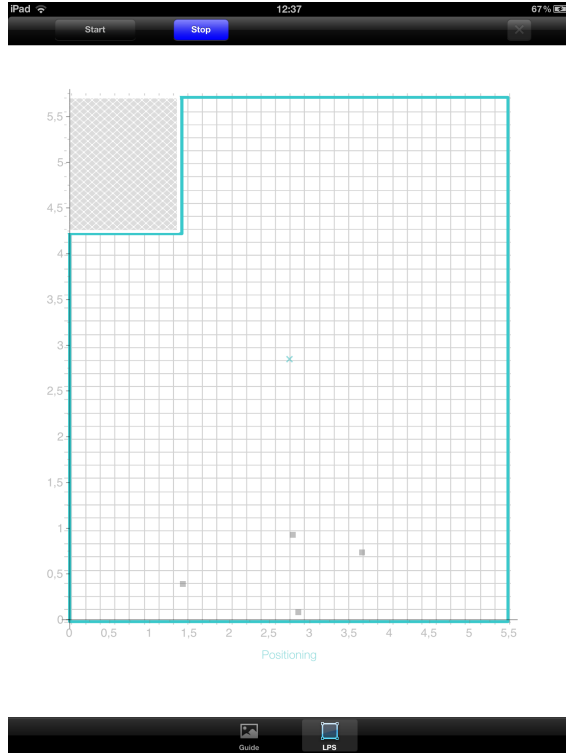


Fig. 13. Screenshot of the LPS user interface.

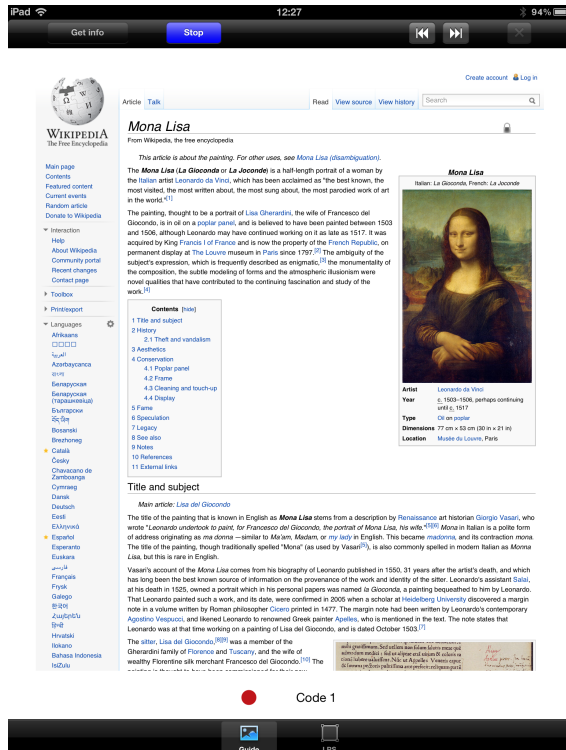


Fig. 14. Screenshot of the LBS user interface.

After data acquisition and processing to calculate the position of the user, this information is displayed through an user interface. The interface consists of two tabs, which are illustrated in Figs. 13 and 14.

The first tab shown in Fig. 13 describes the plane of the laboratory where the tests are performed. The location of the beacons (gray squares), and the estimated position of the user (cyan cross) can be distinguished at every moment. Also a *Start/Stop* button and another *Exit* button are necessary to handle the application.

On the second tab shown in Fig. 14, the user can receive information when being close to one of the beacons. This tab consists of a *User Interface Web View (UIWebView)*, a *Start/Stop* button, controls for surfing the internet and finally an *Exit* button. As shown in this figure, the *iPad* has detected the emission of *Code 1*. The speaker which emits *Code 1* is supposed to be near the painting associated with this code, i.e. *The Gioconda*. After detection of *Code 1*, the application load a *URL* where the user is informed about the painting of *The Mona Lisa*. When the user approaches another picture, a new code is detected and immediately the *iPad* will display information via web page regarding the new painting, since every code has associated its own *URL* address.

### V. CONCLUSIONS AND FURTHER WORKS

In this work the ability of iPhone or iPad to acquire ultrasonic signals around 20 KHz and its possible use for accurate ultrasonic code identifying, it has been successfully developed. The implementation of an ultrasonic local positioning system has been carried out favorably. In addition, it has been made an study on the accuracy and reliability of the system at certain positions in the working environment. These results show that for a total of 100 measurements in each of the positions studied, the error vary between 0.03 and 0.9 meters in the best and worst of the cases respectively, depending on the user's location. In this way for the determination of the TOF in locations where the received signal is not affected by multipath or / and near-far effect, the accuracy of the system significantly improves respect to areas affected by these phenomena, such as corners or at positions very close to the beacons or walls.

Besides, a code-detection related utility has been developed, displaying information to the users through a web page. This utility benefits from near-far effect to detect when the user is close to a beacon offering him LBS related with beacon's location.

Facing further work we are developing improvements related with emitted codes from the point of view of dynamic thresholding, as well as their Doppler effect tolerance when the users are moving.

### ACKNOWLEDGMENTS

This work has been supported jointly by the University of Extremadura through its Aid Program for Initiation in Research (ACCVII-11), and the Spanish Ministry of Economy and Competitiveness, through the project LORIS-UEx (TIN2012-38080-C04-02).

## REFERENCES

- [1] P. Zandbergen, "Accuracy of iphone locations: A comparison of assisted gps, wifi and cellular positioning," *Transactions in GIS*, vol. 13, pp. 5–26, 2009.
- [2] R. Want, A. Hopper, V. Falçao, and J. Gibbons, "The active badge location system," *ACM Transactions Information systems*, pp. 91–102, 1992.
- [3] J. Blankenbach, A. Norrdine, H. Hellmers, and E. Gasparian, "A novel magnetic indoor positioning system for indoor location services," *Proceedings*, 2001.
- [4] A. Bilke and J. Sieck, "Using magnetic field for indoor localisation on a mobile phone," *Progress in Location-Based Services*, 2013.
- [5] K. C. Cheung, S. S. Intille, and K. Larson, "An inexpensive bluetooth-based indoor positioning hack," 2006.
- [6] D. Gusenbauer, C. Isert, and J. Krösche, "Self-contained indoor positioning on off-the-shelf mobile devices," *Proceedings of International Conference on Indoor Positioning and Indoor Navigation (IPIN)*, 2010.
- [7] C. Lukianto, C. Hönniger, and H. Sternberg, "Pedestrian smartphone-based indoor navigation using ultra portable sensory equipment," *Proceedings of Conference on Indoor Positioning and Indoor Navigation (IPIN)*, 2010.
- [8] P. Bahl and V. N. Pandmanabhan, "Radar: An in-building rf-based user location and tracking system," *IEEE Infocom*, pp. 775–784, 2000.
- [9] Y. Inoue, A. Sashima, and K. Kurumatani, "Indoor positioning system using beacon devices for practical pedestrian navigation on mobile phone," *Lecture Notes in Computer Science*, pp. 251–265, 2009.
- [10] T. Gallagher, B. Li, A. G. Dempster, and C. Rizos, "A sector-based campus-wide indoor positioning system," *Proceedings of Conference on Indoor Positioning and Indoor Navigation (IPIN)*, 2010.
- [11] K. Kaemarungsi and P. Krishnamurthy, "Properties of indoor received signal strength for wlan location fingerprinting," *Proceedings of MobiQuitous*, pp. 14–23, 2004.
- [12] A. Ward, A. Jones, and A. Hopper, "A new location technique for the active office," *IEEE Personal Communications*, pp. 42–47, 1997.
- [13] N. B. Priyantha, A. Chakraborty, and H. Balakrishnan, "The cricket location-support system," *Proceedings of ACM Mobicom*, 2000.
- [14] M. Hazas and A. Ward, "A novel broadband ultrasonic location system," *Proceedings of UbiComp 2002: Fourth International Conference on Ubiquitous Computing*, vol. 2498, pp. 264–280, 2002.
- [15] A. Mandal, C. V. Lopes, T. Giavargis, A. Haghighat, R. Jurdak, and P. Baldi, "Beep: 3d indoor positioning using audible sound," *Proceedings of IEEE Consumer Communications and Networking Conference*, January 2005.
- [16] A. Madhavapeddy, D. Scott, and R. Sharp, "Context-aware computing with sound," *Proceedings of Ubicomp*, 2003.
- [17] V. Filonenko, C. Cullen, and J. Carswell, "Investigating ultrasonic positioning on mobile phones," 2010.
- [18] F. Álvarez, T. Aguilera, J. A. Fernández, J. A. Moreno, and A. Gordillo, "Analysis of the performance of an ultrasonic local positioning system based on the emission of kasami codes," *In Proceedings of 2010 International Conference on Indoor Positioning and Indoor Navigation (IPIN)*, 2010.
- [19] P. Bihler, P. Imhoff, and A. B. Cremers, "Smartguide -a smartphone museum guide with ultrasound control," *Procedia Computer Science*, pp. 586–592, 2011.
- [20] T. Kasami, "Weigh distribution formula for some class of cyclic codes," *Technical Report R-285*, 1968.
- [21] "<https://developer.apple.com/xcode/>"
- [22] C. Shannon, "Communication in the presence of noise," *Proceedings of IRE*, pp. 10–21, 1949.